DE GRUYTER OPEN Open Astron, 2017: 26: 233-239

Research Article

Evgenii O. Vasiliev* and Yuri A. Shchekinov

Star formation in shells of colliding multi-SNe **bubbles**

https://doi.org/10.1515/astro-2017-0021 Received Sep 14, 2017; accepted Nov 16, 2017

Abstract: It is believed that when bubbles formed by multiple supernovae explosions interact with one another, they stimulate star formation in overlapping shells. We consider the evolution of a shocked layer formed by the collision of two identical bubbles each of which originated from OB clusters of \sim 50 members and \sim 50 pc. The clusters are separated by 200-400 pc. We found that depending on evolutionary status of colliding bubbles the shocked layer can either be destroyed into diffuse lumps, or be fragmented into dense clumps: the former occurs in collisions of young bubbles with continuing supernovae explosions, and the latter occurs in older bubble interactions. We argue that fragmentation efficiency in shells depends on external heating; for a heating rate $\lesssim 1.7 \times 10^{-24}$ erg s⁻¹ the number of fragments formed in a collision of two old bubbles reaches several tens at $t \sim 4$ Myr, while a heating rate $\gtrsim 7 \times 10^{-24}$ erg s⁻¹ prevents fragmentation. The clumps formed in freely expanding parts of bubbles are gradually destroyed and disappear on $t\lesssim 1$ Myr, whereas those formed in the overlapping shells survive much longer. Because of this the number of fragments in an isolated bubble begins to decrease after reaching a maximum, while in collision of two old bubbles it fluctuates around 60-70 until longer than $t \sim 5$ Myr.

Keywords: galaxies: ISM – ISM: bubbles – shock waves – supernova remnants

1 Introduction

Core-collapse supernovae (SNe) are related to the final stages in the evolution of massive stars, and are normally mostly clustered in space and time because their progenitors - massive stars - form in OB associations. Overlapping multiple SNe remnants form a collective bubble (e.g., McCray & Snow 1987; McCray & Kafatos 1987), sweeping the ambient gas into a thin cold giant shell. Such shells can fragment into molecular clouds, which in turn may become gravitationally unstable and give rise to the next episode of star formation (McCray & Kafatos 1987). Such structures are widely observed both in dwarf and spiral galaxies (e.g., Egorov et al. 2014, 2017).

This concept arose from a common belief that interaction of a SN shock with the interstellar medium (ISM) enhances the fraction of dense and cold gas in it. This understanding stemmed from early numerical simulations

Corresponding Author: Evgenii O. Vasiliev: Southern Federal University, Stachki Ave. 194, Rostov-on-Don 344090, Russia; Special Astrophysical Observatory, RAS, Nizhnii Arkhyz, Karachaevo-Cherkesskaya Republic 369167, Russia; Email: eugstar@mail.ru Yuri A. Shchekinov: Lebedev Physical Institute of Russian Academy of Sciences, ASC, Moscow 117997, Russia; Raman Research Institute, Sadashiva Nagar, Bangalore 560080, India; Email: yus@asc.rssi.ru

which confirmed that SN shock waves compress and implode gaseous lumps (Woodward 1976; Chevalier 1977). Such lumps are thought to collapse and form protostellar clouds. However, shock compression is always accompanied by mass loss due to stripping, and therefore in order for the clumps collapse after stripping their masses have to be sufficiently high. Thus, one can see that only under certain interrelations between parameters of SNe shock waves (shock velocity, thickness of the cold shell behind the shock and so on) and clumps (e.g., mass, size, density), the interaction of a SNe shell with clumps can stimulate star formation. It is revealed in numerical simulations that not every such interaction of an impinging shock with clumps stimulates star formation. More often clumps or clouds and their ensembles are destroyed by shockwaves (e.g., Klein et al. 1994; Poludnenko et al. 2002; Korolev et al. 2015; Pittard & Parkin 2016).

8

Nearby face-on dwarf galaxies often show a presence of numerous giant bubbles in their ISM (e.g., Bagetakos et al. 2011), in some cases merging with one another (Dawson et al. 2013, 2015; Gaczkowski et al. 2015). Such mergers begin with a collision of their shells which forms a thin cold and dense layer. Quite similar to a shell of an isolated bubble, this layer can give rise to star formation. One may think of collisions of bubbles as a part of generic feedback processes in the ISM: starforming regions produce

bubbles, whose mutual interaction gives rise to molecular clouds, which in turn fragment to form protostars, and so on (Egorov et al. 2014; Inutsuka et al. 2015).

It is commonly believed that dense layers behind colliding interstellar flows result in gravitational fragmentation (Stone 1970; Gilden 1984; Elmegreen & Elmegreen 1978) followed by the formation of molecular clouds (e.g. Heitsch et al. 2006). In simulations the properties of such interacting flows are usually assumed to be close to values typical of the warm ISM: a density of $n \sim 0.1 - 1 \text{ cm}^{-3}$ and a velocity of $10 - 30 \text{ km s}^{-1}$ (e.g. Heitsch et al. 2006; Hennebelle 2013).

These differ from those taking place in the collision of bubbles. At the initial phase cold and dense (of $\sim M^2 n$, where M is the Mach number and n is number density before the shock wave) shock compressed shells meet with velocities of several tens of km s⁻¹ and form a contact discontinuity. Then two diverging shocks propagate in opposite directions to the bulk counterflowing shells, and when they reach their rear the shocks may break into the hot interior of the bubbles, particularly when pressure in the hot interior drops down due to radiative cooling. It depends therefore whether SNe explosions inside the bubbles continue or not. In this scenario the layer formed between the collision of two bubbles can be ultimately destroyed (Chernin et al. 1995). In this case the overall picture of circulation of molecular clouds and star formation in the Milky Way will differ from that proposed by Inutsuka et al. (2015). Thus, the ability of SNe explosions to enhance star formation depends on details of gas dynamics in the layers between their overlapping shells. The collision of two bubbles has been considered numerically in 2D (Ntormousi et al. 2011), and recently in 3D magneto-hydrodynamic models in (Ntormousi et al. 2017), where properties of cloudlets formed in merging superbubbles under continuous energy input are described in detail. However, the dynamics of the shells of merging superbubbles is dependent on whether energy input from the SNe explosion still continues to feed the superbubbles or they merge under the conditions of already exhausted explosions. This still remains unexplored. Moreover, Ntormousi et al. (2017) limited their description to before the merged supershells become breaking and pervading - a catastrophic change of their dynamical state.

In this paper we investigate the evolution of a layer formed in the collision of two identical bubbles. Section 2 describes our model. Section 3 presents the results and Section 4 summarizes our conclusions.

2 Description of the model

We carry out 3D hydrodynamic simulations (Cartesian geometry) of a collision of two bubbles formed by multiple SNe explosions clustered in space. We consider bubbles of the same age. The number of massive stars, the SN progenitors, in each cluster is 50. The stars are distributed uniformly and randomly inside a region with a fixed cluster radius $r_c = 50$ pc, which is typical for OB association size. Their masses M are distributed within the range 20-40 M_{\odot} according to a Salpeter initial mass function. SNe in a cluster explode one by one depending on their lifetime: $\log (t_1, \text{yr}) = 10.04 - 3.8054 \log M + 1.0646 \log^2 M$ (Iben 2012), so that all SNe have exploded ~ 3 Myr after the first SN event. We inject the mass and the energy of each SN into a region of radius $r_0 = 3$ pc. The SN energy 10⁵¹ erg is injected in thermal form. The ambient gas density is 1 cm^{-3} and the temperature is $3 \times 10^3 \text{ K}$; gas metallicity is kept constant and equal to the solar value within the whole computational domain.

Standard simulations are performed with a physical cell size of 2 pc throughout the computational domain. We describe the collision between the bubbles at different evolutionary phases: 1) the merging occurs when about 0.5 Myr remained for the SNe to exhaust, and 2) the merging begins about 1 Myr after SNe explosions in the bubbles have been exhausted. We fit the computational domain sizes to these two cases.

The code is based on the unsplit total variation diminishing (TVD) approach that provides high-resolution capturing of shocks and prevents unphysical oscillations. We have implemented the Monotonic Upstream-Centered Scheme for Conservation Laws (MUSCL)-Hancock scheme and the Haarten-Lax-van Leer-Contact (HLLC) method (see e.g. Toro 1999) as an approximate Riemann solver. This approach has successfully passed the whole set of tests proposed in Klingenberg et al. (2007).

Simulations are run including radiative cooling processes with a tabulated non-equilibrium cooling curve fitting the calculations (Vasiliev 2011, 2013) for a gas cooling isochorically from 10^8 down to 10 K. The non-equilibrium cooling rate (Vasiliev 2011, 2013) includes kinetics of all ionization states of H, He, C, N, O, Ne, Mg, Si, and Fe, as well as kinetics of molecular hydrogen at $T < 10^4$ K. In our fiducial simulations heating rate is assumed to be constant at $G = 1.7 \times 10^{-24}$ erg s⁻¹ chosen as such to stabilize the radiative cooling of the ambient unperturbed gas at $T = 3 \times 10^3$ K, but we also consider several other values for the heating rate. The equilibrium between cooling and externally stabilizing heating G is violated when gas den-

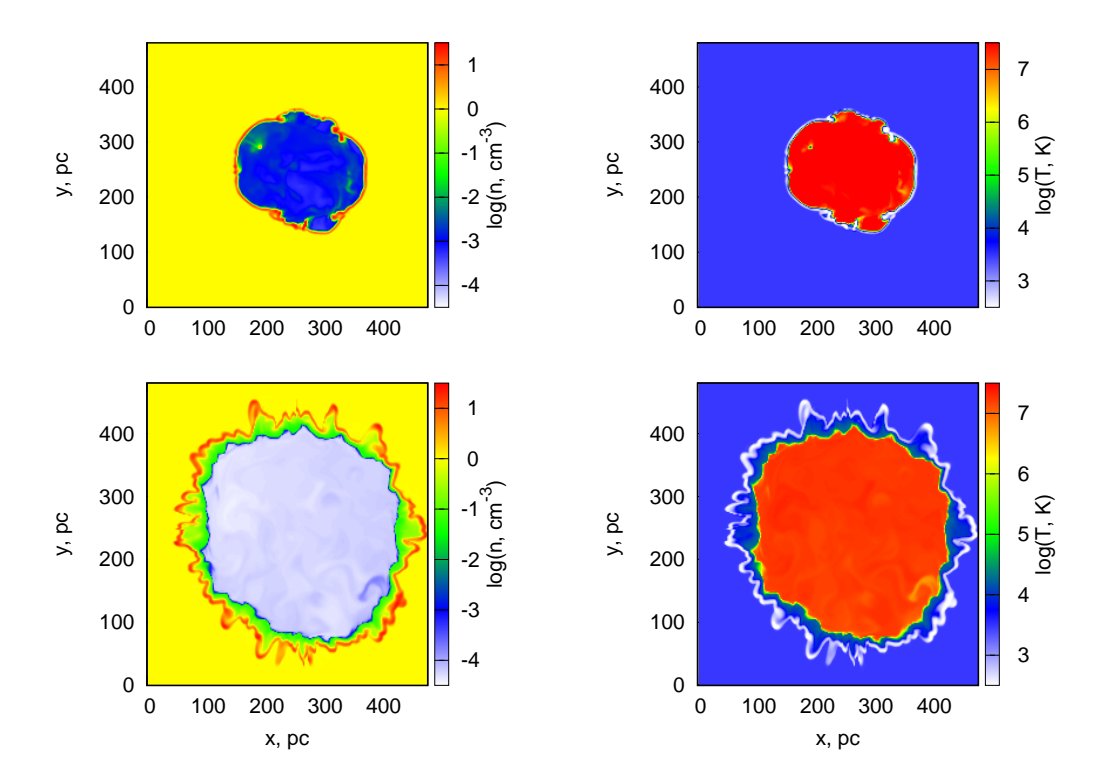


Figure 1. The density (left column) and temperature (right column) slices at z = 250 pc for isolated bubble formed by multiple SN explosions in a cluster at time moments 2 Myr (upper panels) and 6 Myr (lower panels).

sity and temperature deviate from the equilibrium state by more than 1%.

3 Results

3.1 Dynamics of isolated bubble

At first we briefly outline the evolution of an isolated bubble in a homogeneous medium. Multiple SNe which exploded in an OB cluster interact with each other and form a collective bubble (e.g., Yadav et al. 2017; Vasiliev et al. 2017). This bubble expands as a wind driven shell with $r \sim t^{3/5}$ (Avedisova 1972; Castor et al. 1975) while SNe continue to explode. The expanding shell cools down, becoming denser and unstable. The energy source driving the wind exhausts when the least massive stars $(M = 8M_{\odot})$ explode as SNe. After that the shell decelerates faster, because gas pressure in the hot bubble drops due to radiative cooling. Under such conditions instabilities develop more efficiently and can give rise to fragmentation. Figure 1 presents the density and temperature slices at z = 250 pcfor an isolated bubble formed by multiple SN explosions in a cluster. The upper panel corresponds to the moment when SNe are still exploding, whereas the lower presents the state when all SNe have exhausted and the shell becomes well-fragmented.

3.2 Dynamics of merging bubbles

Because of the high density of stars in starforming regions the SNe remnants merge, forming collective bubbles. They grow under continuous energy injection from the next generation of SNe and after a certain time can in turn merge on large scales with similarly growing bubbles in their neighbourhood (e.g., de Avillez 2000). When two such bubbles merge their shells form in the interaction zone a layer with nearly double the surface density, which makes conditions in this interaction region favourable for subsequent star formation (Inutsuka et al. 2015). Such dense layers between merged bubbles are immersed into hot low-density interiors of the bubbles, and therefore the dynamics of the layer is fully dependent on the physical conditions of the bath of surrounding bubbles: the temperature and density, velocity field, regime of energy injection from SNe and so on. For instance, it looks obvious that the dynamical state of the layer formed by a merger between young bubbles with continuous SNe explosions will differ from that

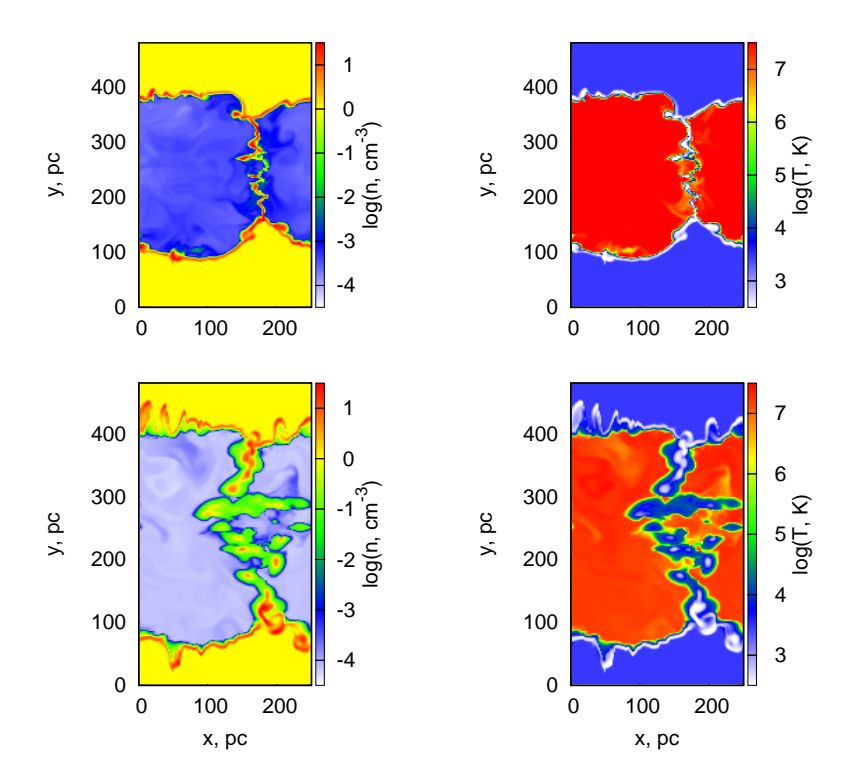


Figure 2. The density (left column) and temperature (right column) slices of the region, where two bubbles collide, at time moments 3.5 Myr (upper panels) and 5.5 Myr (lower panels). The collision occurs, when the age of each bubble is 2.5 Myr.

formed by older ones in which SNe are exhausted. For the sake of specificity we restrict our consideration here to the description of a merger of two bubbles of equal age.

Figure 2 shows the density (left column) and temperature (right column) slices of the region, where two bubbles merge, at time moments 3.5 Myr (upper panel) and 5.5 Myr (lower panel) since the first SN explosion. The bubbles merged when their age was about 2.5 Myr, so that the slices shown in Figure 2 correspond to about 1 Myr and 3 Myr since the bubbles have merged. By this time SNe explosions in each bubble had already exhausted, and as a consequence the expansion velocity of their shell turned to decrease faster than $v \sim t^{-2/5} \sim r^{-2/3}$. This means that the earlier the merging takes place the higher velocity of the colliding shells is. By the time of merging the shells are as a rule on the radiative phase, and the cooling gas turns to be fragmenting into small clumps due to thermal instability enhanced by hydrodynamical instabilities. Fragmentation is a common phenomenon in young bubbles, however thermal instability makes the shell thin and results usually in small size cloudlets. Along with a non-central and randomly spread SNe explosions efficient cooling leads to a distorted shape of the shells, and the cold heavily compressed interfacial layer between the merging bubbles is bending immediately after the shells come into contact.

On the upper panel of Figure 2 one can see a thin heavily distorted layer. Strongly growing density variations result eventually in breaking the compressed layer (e.g. Chernin et al. 1995), which is clearly seen at a later time as shown in the lower panel. From the hot interior of the bubbles outward, the cold layer gradually cools down and causes the pressure to decrease, thus enhancing destruction of the cold layer.

Even though slowly expanding older bubbles seem intuitively to be stable against destruction, the overall picture is less obvious. The total mass involved into the cooling compressing layer is in this case higher due to a higher amount of swept up mass. A progressive cooling of shocked gas goes on, and as far as the expansion velocity is higher than around $\gtrsim 30 \, \mathrm{km \, s^{-1}}$ and the postshock temperature is higher than $\gtrsim 10^4$ K it initiates thermal instability and gas fragmentation. Figure 3 shows the density (left column) and temperature (right column) slices of the merger region at 5.5 Myr (upper panel) and 7 Myr (lower panel) after SNe explosions have begun in the cluster. Contrary to the models shown above here the bubbles merge when their age is about 4.3 Myr, so that the snapshots in Figure 3 correspond to about 1.2 Myr and 2.7 Myr since the shells contacted. On the upper panel a well-fragmented cold shell is clearly seen. In the collision plane the cold-

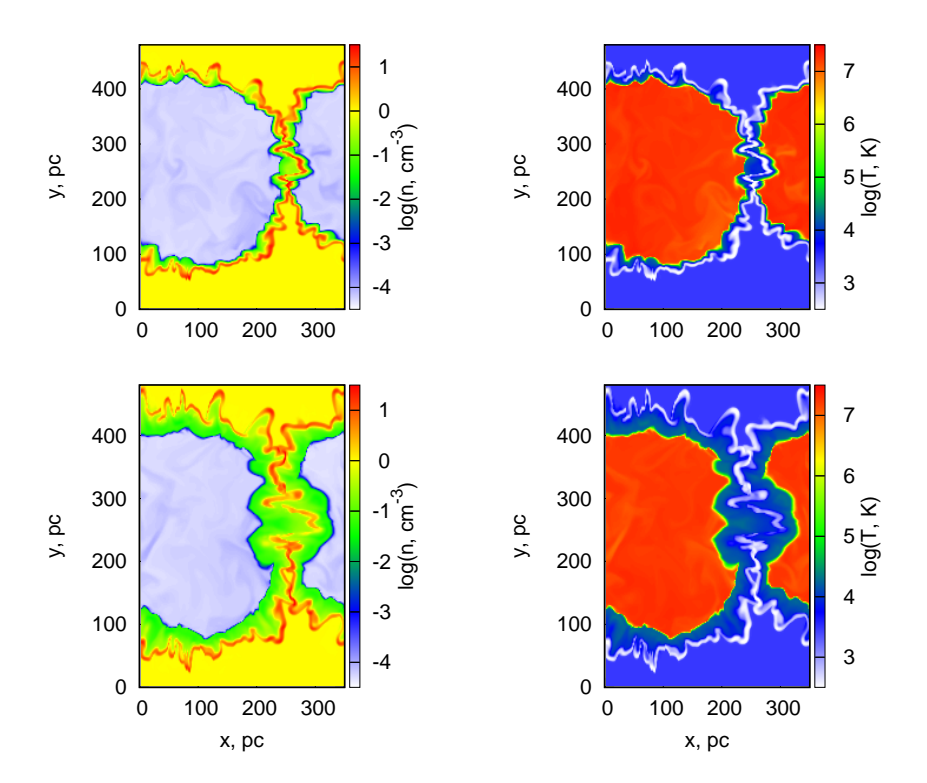


Figure 3. The density (left column) and temperature (right column) slices of the region, where two bubbles merge, at time moments 5.5 Myr (upper panels) and 7 Myr (lower panels). At the time of collision the age of each bubble is 4.3 Myr.

est layer with $T \lesssim 500$ K is immersed into diffuse gas with $T \sim 10^4$ K. This layer is generally thicker than that formed in younger merging bubbles (Figure 2). Moreover, the cold layer is kept even after 2.7 Myr since the first shells contact (see the lower panel). Thus, the destruction of the cold layer is less effective for the collision of older bubbles.

3.3 Statistics of fragments

During the expansion of even an isolated bubble its shell experiences distortion and fragmentation into cold and dense clumps. A few of them can survive, and might become gravitationally unstable in further evolution. However, ram pressure stripping works as a rule to destroy them efficiently. In the shells of merging bubbles pressure is higher, and it favours gas to reach lower temperatures and higher densities. Under such conditions the fragments might survive longer and become gravitationally unstable. However, a competitive process is the stripping by ram pressure and variations of external gas pressure, resulting in the creation of multiple diffuse clouds and clumps. The two competitive regimes are represented in Figure 1 where the fragments eventually are destroyed, and in Figures 2

and 3 on the other side where they grow and can asymptotically survive.

We define a clump merely as "an island" of cold and dense gas or, more precisely, a group of cells having a common border where the density and temperature are higher and, respectively, lower than a given limit. The conditions for density and temperature should be fulfilled simultaneously. We apply the following limits: $n > 14 \text{ cm}^{-3}$ and T < 300 K. These values have been chosen to some extent arbitrary. For instance, a choice of a lower density (a higher temperature) can lead to extraction of extremely large areas comparable in size to the current radius of the bubbles. At the same time, in case of a higher density (lower temperature) threshold a fraction of cells in the extracted fragments show too small sizes to consider this collection of such cells to belong to the same physical object. In our analysis we take into account clumps with the number of cells larger than 100.

The process of fragmentation of dense expanding shells and physical characteristics of the formed fragments depends on many factors. Among others, the velocity field in the shell is determining. Thus, as soon as motions in a quasi-spherical shell of a single bubble are mostly diverging, the instabilities driving the shell fragmentation at the early stages, will weaken because

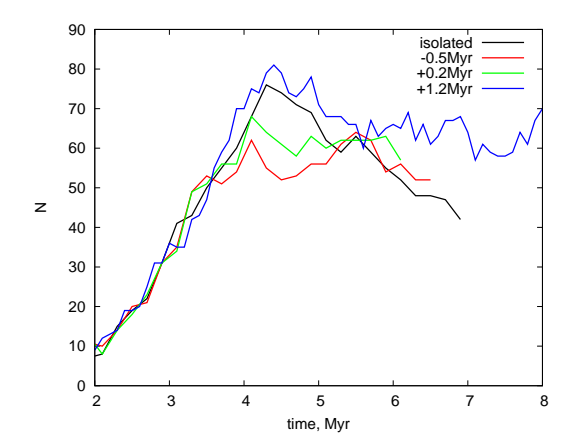


Figure 4. Number of cold and dense fragments in the isolated bubble (black line) and two colliding bubbles depending on the age of the bubbles: (a) SNe explosions exhausted 0.5 Myr after the merging (label '-0.5Myr', red line), (b) SNe exhausted 0.2 Myr before the merging (label '+0.2Myr', green line), (c) SNe exhausted 1.2 Myr before the merging (label '+1.2Myr', blue line). The value along the x-axis is the age of the bubbles.

growing instabilities become inefficient at replenishing the number of fragments. Eventually most of the fragments will disappear. In all considered models the growing clumps begin forming when the bubble age is about 2 Myr. Their further evolution is depicted in Figure 4. The black line shows the total number of such clumps in the fragmenting shells of an isolated bubble (see Figure 1). This number grows, reaches maximum at $t \sim 4$ Myr, and then turns to decrease.

On the contrary, in a shell of a quasi-planar symmetry formed by the merging of two nearly equal bubbles, the velocity field is mainly converging on initial stages after the merging and, particularly, in the regions where the two shells contact. This circumstance tends to allow the clumps to survive. However, another factor to diminish the number of growing clumps comes soon into play – the destruction of the shell by instabilities driven by high pressure from the hot interior of the bubbles. These instabilities result in chaotic flows highly diverging on small scales and disintegrating the shell itself. In such conditions thermal instability is inhibited and cannot maintain the growth of fragments. As a result, the number of clumps in the shell of two merging bubbles also decreases on longer timescales.

Fragment production by thermal instability compete for their disruption with random diverging flows in the region of a common shell, where the hot interior of merged bubbles, eventually breaks the compressed shell and intermittently penetrates each other. This phenomenon is more efficient with the bubbles in which continuing SNe explo-

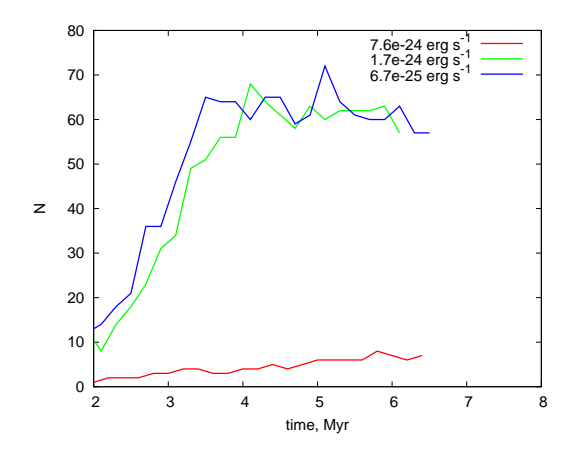


Figure 5. Number of cold and dense fragments in two bubbles collided about 0.2 Myr after all SNe have exploded in the bubbles for different background heating rate (or background temperature) values: $G=7.6\times10^{-24}~{\rm erg~s^{-1}}$ ($T_b=10^4~{\rm K}$) – red line, $G=1.7\times10^{-24}~{\rm erg~s^{-1}}$ ($T_b=3\times10^3~{\rm K}$) – green line, $G=6.7\times10^{-25}~{\rm erg~s^{-1}}$ ($T_b=10^3~{\rm K}$) – blue line. The value along the x-axis is the age of the bubbles.

sions still add energy. Such a difference can be observed in Figure 4, where red and green lines depict how the number of fragments varies in time depending on whether the bubbles merged before or after the energy source - exploding SNe - is exhausted. In the first case (red line) when bubbles merge SNe in them explode and become exhausted only 0.5 Myr later. In the second (blue line) the merging occurs when the stars are already inactive after 1.2 Myr and do not add mechanical energy into the bubbles. The inactive bubble (blue line) produces larger number of fragments, which peaks at $\simeq 4.5$ Myr and then starts decreasing. This decrease continues until ~ 6 Myr or about 1.5 Myr after the merging has started. After that the number of fragments almost saturates around 65. Also we present the intermediate case, where SNe became inactive almost just after the merging has occurred (green line). One can see that the number of fragments is slightly higher than that in the model, where stars are still active after merging (red line).

External heating plays obviously a crucial role in the evolution of gravitationally stable clumps: higher heating rate leads to warmer and less dense gas in the shell. The number of fragments decreases for a higher heating rate, that is clearly seen in Figure 5. There exists a critical value of the heating rate which prevents the formation of fragments. In the model we presented it is $G \gtrsim 7 \times 10^{-24}$ erg s⁻¹.

4 Conclusion

In this paper we consider the evolution of colliding bubbles formed by multiple SNe explosions in the uniform background with number density equal to 1 cm⁻³ and the metallicity is assumed to be equal to the solar value. For the sake of simplicity we constrain only by the interaction of two identical bubbles, i.e. having both the same age and same number of SNe events. We assume an OB cluster consists of ~ 50 massive stars enclosed in ~ 50 pc. We are interested in how fragmentation is effective in colliding bubbles compared to isolated ones.

We have found that depending on evolutionary status of colliding bubbles a gaseous layer formed in the collision place can either be destroyed into diffuse lumps or be able to fragment into dense clumps: the former takes place in the collision of young bubbles or in which SNe explosions continue to explode, the latter occurs in case of older (more than 1 Myr after SNe explosions have ceased) bubble interaction.

During the expansion of bubbles the shell can be fragmented into numerous cold and dense clumps. For heating rate $G \lesssim 1.7 \times 10^{-24} \text{ erg s}^{-1}$ the number of fragments after a collision of two old bubbles reaches several tens at $t \sim 4$ Myr. Further, the clumps are gradually destroyed in the freely expanding parts of bubbles. Eventually, the number of fragments grown in an isolated bubble decreases after reaching a maximum. On the contrary, the number of fragments in a collision of two old bubbles fluctuates around 60-70 after $t \sim 5$ Myr. External heating with a rate as high as $G \gtrsim 7 \times 10^{-24} \text{ erg s}^{-1}$ prevents formation of fragments in bubbles.

Acknowledgment: The numerical simulations were performed under support from the Russian Scientific Foundation (grant 14-50-00043). EV is grateful to the Ministry for Education and Science of the Russian Federation (grant 3.858.2017/4.6). YS is partially supported by the RFBR (grants 15-02-08293, 17-52-45053).

References

Avedisova, V.S. 1972, SvA, 15, 708-713.

Bagetakos, I., Brinks, E., Walter F., de Blok, W.J.G., Usero, A., Leroy, A. K. et al., 2011, AJ, 141, 23.

Castor J., McCray, R. and Weaver, R. 1975, ApJL, 200, 107-110.

Chernin, A.D., Efremov, Yu.N., Voinovich, P.A. 1995, MNRAS, 275, 313-326.

Chevalier, R. 1977, 1977, ARA&A, 15, 175-196.

Dawson, J.R., McClure-Griffiths, N. M., Wong, T., Dickey, John M., Hughes, A., Fukui, Y. et al., 2013, ApJ, 763, 56.

Dawson J.R., Ntormousi E., Fukui Y., Hayakawa T., and Fierlinger K., 2015, ApJ, 799(1), 64.

de Avillez, M.A. 2000, MNRAS, 315, 479-497.

Egorov, O.V., Lozinskaya, T.A., Moiseev, A.V., and Smirnov-Pinchukov, G.V. 2014, MNRAS, 444, 376-391.

Egorov, O.V., Lozinskaya, T.A., Moiseev, A.V., and Shchekinov, Yu. A. 2017, MNRAS, 464, 1833-1853.

Elmegreen, B.G. and Elmegreen, D.M. 1978, ApJ, 220, 1051-1062.

Gaczkowski, B., Preibisch, T., Stanke, T., Krause, M.G.H., Burkert A., Diehl, R. et al., 2015, A&A, 584, 36.

Gilden, D.L. 1984, ApJ, 279, 335-349.

Heitsch, F., Slyz, A.D., Devriendt, J.E.G., Hartmann, L. W., and Burkert, A. 2006, ApJ, 648(2), 1052-1065.

Hennebelle, P. 2013, A&A 556, 153.

Iben, I. 2012, Stellar Evolution Physics, Volume 2, Cambridge, Cambridge University Press.

Inutsuka, Sh., Inoue, T., Iwasaki, K., and Hosokawa, T. 2015, A&A, 580, 49.

Klein, R.I., McKee, C.F., and Colella, P. 1994, ApJ, 420, 213-236.

Klingenberg, Ch., Schmidt, W., Waagan, K. 2007, J. Comp. Phys., 227, 12-35.

Korolev, V. V., Vasiliev, E.O., Kovalenko, I.G., Shchekinov, Yu.A., 2015, ARep, 59, 690-708.

McCray, R. and Snow-T. P. Jr. 1979, Ann. Rev. Astron. Ap., 17, 213-

McCray, R. and Kafatos, M. 1987, ApJ, 317, 190-196.

Ntormousi, E., Burkert, A., Fierlinger, K., and Heitsch, F. 2011, ApJ, 731, 13.

Ntormousi, E., Dawson, J.R., Hennebelle, P., Fierlinger, K. 2017, A&A, 599, 94-109.

Pittard J.M. and Parkin, E.R. 2016, MNRAS, 457, 4470-4498.

Poludnenko, A.Y., Frank, A., and Blackman, E.G. 2002, ApJ, 576, 832-848.

Stone, M.E. 1970, ApJ, 159, 277-292.

Toro, E. 1999, Riemann solvers and numerical methods for fluid dynamics, Springer-Verlag, Berlin, Second Edition.

Vasiliev, E.O. 2011, MNRAS, 414, 3145-3157.

Vasiliev, E.O. 2013, MNRAS, 431, 638-647.

Vasiliev, E.O., Nath, B.B., Shchekinov, Yu.A. 2017, MNRAS, 468, 2757-2770.

Woodward, P.R. 1976, ApJ, 207, 484-501.

Yadav, N., Mukherjee, D., Sharma, P., and Nath, B.B., 2017, MNRAS, 465, 1720-1740.